Published in final edited form as:
Chem Biol. 2009 July 31; 16(7): 744–753. doi:10.1016/j.chembiol.2009.05.009.

Characterization of monoacylglycerol lipase inhibition reveals differences in central and peripheral endocannabinoid metabolism

Jonathan Z. Long[1], **Daniel K. Nomura**[1], and **Benjamin F. Cravatt**[1,†]

[1] The Skaggs Institute for Chemical Biology and Department of Chemical Physiology, The Scripps Research Institute, 10550 N. Torrey Pines Rd. La Jolla, CA 92037

SUMMARY

Monoacylglycerol lipase (MAGL) is a principal degradative enzyme for the endocannabinoid 2-arachidonoylglycerol (2-AG). We recently reported a piperidine carbamate, JZL184, that inhibits MAGL with high potency and selectivity. Here, we describe a comprehensive mechanistic characterization of JZL184. We provide evidence that JZL184 irreversibly inhibits MAGL via carbamoylation the enzyme's serine nucleophile. Functional proteomic analysis of mice treated with JZL184 revealed that this inhibitor maintains good selectivity for MAGL across a wide range of central and peripheral tissues. Interestingly, MAGL blockade produced marked, tissue-specific differences in monoglyceride metabolism, with brain showing the most dramatic elevations in 2-AG and peripheral tissues often showing greater changes in other monoglycerides. Collectively, these studies indicate that MAGL exerts tissue-dependent control over endocannabinoid and monoglyceride metabolism and designate JZL184 as a selective tool to characterize the functions of MAGL in vivo.

INTRODUCTION

Monoacylglycerol lipase (MAGL) is a 33-kDa, peripherally associated membrane enzyme of the serine hydrolase superfamily that catalyzes the hydrolysis of monoacylglycerols (MAGs) to free fatty acid and glycerol [1,2]. MAGL contains the classical G*X*S*X*G consensus sequence common to most serine hydrolases and is predicted by sequence homology to have an α/β-hydrolase fold. The catalytic triad has been identified as Ser122, His269, and Asp239 [2]. Though MAGL can hydrolyze 1(3)- and 2-MAGs equally efficiently, it has an exquisite substrate preference for MAGs over triacylglycerols (TAGs) and diacylglycerols (DAGs) [1, 3]. Beyond its initially described contribution to lipolysis in adipose tissue, MAGL has also been proposed to degrade the endogenous cannabinoid (endocannabinoid) 2-arachidonoylglycerol (2-AG) [4,5] in the nervous system [6]. 2-AG, along with a second endocannabinoid anandamide (AEA) [7], are signaling lipids that activate the cannabinoid receptors CB1 [8] and CB2 [9], two G-protein coupled receptors that also mediate the neurobehavioral and immunosuppressive effects of the pyschoactive component of marijuana, Δ^9-tetrahydocannabinol (THC) [10–12]. Endocannabinoids have been implicated in the regulation of a number of (patho)physiological processes that reflect functions in both the nervous system (e.g., pain, anxiety, cognition) and peripheral tissues (e.g., dyslipidemia, inflammation, fertility) [10,13].

†To whom correspondence should be addressed: cravatt@scripps.edu.

Endocannabinoid signaling is terminated by enzymatic hydrolysis, a process that, for AEA, occurs by the action of fatty acid amide hydrolase (FAAH) [14,15]. Although several enzymes have been implicated in the hydrolysis of 2-AG, we and others have provided evidence that MAGL is the principal 2-AG hydrolase in rodent brain [6,16–19]. To investigate the role that MAGL plays in endocannabinoid metabolism and signaling in vivo, we recently described a potent and selective inhibitor of this enzyme termed JZL184 [20] that, upon administration to mice, decreased brain MAG hydrolysis activity by up to 85% and dramatically elevated brain 2-AG levels. These biochemical and metabolic changes were accompanied by several CB1-dependent behavioral phenotypes, including hypomotility, hypothermia, and analgesia. Key to the development of JZL184 was the implementation of competitive activity-based protein profiling (ABPP) screens [21,22] to direct the concurrent optimization of inhibitor potency and selectivity. Here, we extend this initial study by presenting a detailed mechanistic characterization of JZL184. We provide evidence that JZL184 inhibits MAGL by carbamoylation of the enzyme's active site serine nucleophile. We also demonstrate that JZL184 can be used to globally inactivate MAGL in both central and peripheral tissues, where the inhibitor maintains good selectivity, showing only a handful of off-targets in a select subset of tissues. Interestingly, we observed marked tissue-specific differences in the accumulation of 2-AG and other MAG species upon MAGL inhibition, suggesting that endocannabinoid tone and its regulation by MAGL vary across individual organs.

RESULTS

JZL184 inhibits MAGL by irreversible active-site carbamoylation

Carbamate inhibitors typically inactivate serine hydrolases by irreversible (or slowly reversible) covalent modification (carbamoylation) of the catalytic serine nucleophile [23,24] (Figure 1A). We therefore sought to test whether this mechanism was operational for inhibition of MAGL by JZL184. JZL184-treated and DMSO-treated (control) preparations of purified MAGL were digested with trypsin and analyzed by liquid chromatography tandem mass spectrometry (LC-MS/MS) on a high-resolution instrument (LTQ-Orbitrap). We searched the resulting MS1 (parent ion) profiles for masses corresponding to the unmodified and carbamoylated forms of the MAGL active site peptide. In control samples without inhibitor, we observed a single peak with m/z = 1312.96, corresponding to the 4+ charge state of the unmodified MAGL active site tryptic peptide, amino acids 110–160. In samples treated with JZL184, a new peak appeared with m/z = 1408.24, corresponding to the 4+ charge state of the carbamoylated form of the active site peptide (Figure 1B). The detected adduct was unique to the active site peptide, since an analysis of other tryptic peptides derived from MAGL revealed no evidence of JZL184 adducts (Figure S1). MS/MS analysis of the unmodified and JZL184-modified forms of the active site peptide identified six common y^{1+} fragment ions (Figure 1C). Notably, the active site peptide contains three serine residues, and two of these serines are detected in unmodified form in the $y15^{1+}$ and $y16^{1+}$ MS/MS fragment ions for both control and JLZ184-treated MAGL preparations (Figure 1C). The remaining serine, which is located in the portion of the active site peptide modified by JZL184, corresponds to the predicted catalytic nucleophile Ser122, based on previous studies [2] and the complete conservation of this residue across all MAGL orthologues and distantly homologous serine hydrolases. We therefore recombinantly expressed and purified a MAGL mutant in which the catalytic Ser122 was mutated to an alanine (MAGL-S122A). Upon incubation with JZL184, digestion with trypsin, and LC-MS/MS analysis, we detected a single peak with m/z = 1308.96 corresponding to the unmodified MAGL-S122A active site tryptic peptide, but did not detect a peak corresponding to the JZL184-adduct of this peptide (Figure S2). Collectively, these data indicate that JZL184 inactivates MAGL by covalent carbamoylation of the enzyme's catalytic nucleophile Ser122.

To assess the stability of the JZL184-MAGL adduct, we measured the rate of decarbamoylation of this complex by incubating recombinant MAGL overexpressed in COS7 cells with JZL184 and then using size-exclusion chromatography to remove unreacted JZL184. MAGL activity was then measured by 2-AG hydrolysis assays over a period of 30 h at room temperature. Less than 10% recovery of enzyme activity was observed over this period (Figure 1D), indicating that the JZL184-MAGL adduct is very stable.

An optimized vehicle delivery system for in vivo analysis of JZL184

In our initial disclosure of JZL184, we administered the compound intraperitoneally (i.p.) to mice in a polyethylene glycol (PEG) vehicle [20] because this vehicle best solublized JZL184 (Figure S3). However, we have found that the PEG vehicle can confound certain metabolomic measurements, especially in peripheral tissues where PEG can accumulate and reside for extended time periods. Owing to the popularity of saline-emulphor vehicles for delivering inhibitors and other xenobiotics [25–28], we explored the possibility of administering JZL184 in an 18:1:1 solution of saline:emulphor:ethanol. Simple addition of JZL184 to this vehicle resulting in poor solubility and in vivo activity (as judged by lack of MAGL inhibition in brain tissue; data not shown). However, extensive sonication of JZL184 in the saline-emulphor vehicle was found to produce a uniform suspension (Figure S3) that could be administered to rodents by intraperitoneal injection to efficiently inactivate MAGL in vivo.

We directly compared the PEG and saline-emulphor delivery systems for JZL184 by measuring brain MAGL activity and lipid levels from inhibitor-treated mice. C57Bl/6 mice were treated with JZL184 (4–40 mg kg^{-1}, 18:1:1 saline:ethanol:emulphor vehicle, i.p. or 16 mg kg^{-1}, PEG vehicle, i.p.) and sacrificed after 4 h for analysis. JZL184 in both vehicles produced near-complete and selective blockade of MAGL activity as judged by competitive ABPP with the serine hydrolase-directed probe fluorophosphonate (FP)-rhodamine [29] (Figure 2A) or 2-AG hydrolytic substrate assays (Figure 2B), which was accompanied by dramatic elevations in 2-AG (Figure 2C, *left panel*) and more modest changes in other MAGs such as mono-palmitoylglycerol (C16:0 MAG) and mono-oleoylglycerol (C18:1 MAG) (Figure 2C, *middle panel*). A slightly higher dose of JZL184 was required in the saline-emulphor vehicle to achieve the same 2-AG elevations as observed with the PEG vehicle (40 mg kg^{-1} versus 16 mg kg^{-1}, respectively; Figure 2C, *left panel*). JZL184 showing excellent selectivity in the nervous system, as this agent did not block FP-rhodamine labeling of other brain hydrolases (Figure 2A) and showed only modest inhibition of FAAH activity (~50% at the highest dose tested, Figure 2B) that did not produce changes in brain AEA levels (Figure 2C, *right panel*). These observations are consistent with previous reports that > 85% FAAH inhibition is required to observe bulk changes in AEA levels [27,30], and that a partial blockade of FAAH activity does not alter stimulated AEA production [20]. 2-AG was similarly elevated in FAAH (−/−) mice [15] treated with JZL184 (Figure S4), demonstrating that genetic disruption of FAAH does not alter brain 2-AG metabolism by MAGL.

Consistent with our previous report [20], JZL184 administered in a PEG vehicle was found to cause three of the four behavioral effects of the tetrad test characteristic of direct CB1 agonists, namely, hypomotility (Figure 2D), analgesia (Figure 2E) and hypothermia (Figure 2F), but not catalepsy. Interestingly, a slightly different profile was observed for JZL184 in the saline-emulphor vehicle (40 mg kg^{-1}, i.p., 4 h), where we observed significant CB1-dependent hypomotility (Figure 2G) and analgesia (Figure 2H), but not hypothermia (Figure 2I). The discrepancy in the hypothermic effects of JZL184 administered in different vehicles might be explained in part by the fact that the PEG vehicle alone (but not the saline-emulphor vehicle) caused a transient drop in body temperature, which may suggest that blockade of MAGL causes dysreguation of temperature homeostasis following a hypothermic insult.

Evaluating the inhibition of MAGL in liver by JZL184

We next set out to assess the ability of JZL184 to inhibit MAGL outside of the nervous system. C57Bl/6 mice were treated with JZL184 (16 mg kg^{-1} in saline-emulphor, i.p.), sacrificed at 15 min, 45 min, 2 h, and 4 h post-treatment, and liver tissues removed for analysis. MAGL inactivation in liver, as judged by 2-AG hydrolysis or competitive ABPP assays, was extremely rapid, reaching near-completion by the first time-point analyzed (15 min, Figure 3A). We observed a residual 20% 2-AG hydrolytic activity that was insensitive to JZL184 (Figure 3B), indicating that, like in brain [17, 20], additional enzymes in liver may catalyze this reaction. In contrast to the rapid inactivation of MAGL by JZL184, FAAH was inhibited much more slowly, with ~50% FAAH activity still observed at 4 h post-treatment (Figure 3B). Lipid profiles revealed significant elevations in C20:4, C16:0, and C18:1 MAGs in liver tissue from JZL184-treated mice that peaked between 2–4 h after inhibitor treatment. No changes in AEA levels were detected in liver at any time point post-JZL184 treatment (Figure 3C). C57Bl/6 mice treated with increasing amounts of JZL184 (4–40 mg kg^{-1}, i.p., saline-emulphor, 4 h) showed dose-dependent decreases in MAGL activity by competitive ABPP (Figure 3D) and substrate hydrolysis assays (Figure 3E) that correlated with dose-dependent elevations in liver MAGs (Figure 3F). No changes in liver AEA was observed at any of the doses tested ($P > 0.20$) (Figure 3F).

Competitive ABPP experiments revealed that JZL184 maintained excellent selectivity for MAGL in liver tissue, especially at early time points (< 45 min, 16 mg kg^{-1}) (Figure 3A). At longer time points (4 h; Figure 3A) or higher doses (40 mg kg^{-1}; Figure 3D), we observed a partial decrease in probe labeling signals for multiple proteins in the 50–65 kDa region, which likely correspond to carboxylesterases that are known to be sensitive to a variety of carbamate-based inhibitors [24, 31, 32].

A comprehensive profile of MAGL inactivation in peripheral tissues

The heightened rate and magnitude of accumulation of 2-AG in brain versus liver tissue from JZL184-treated animals suggested that the former tissue exhibits greater capacity to produce this endocannabinoid. To better understand the relative level of endocannabinoid tone across different tissues, we evaluated MAGL activity and lipid profiles in brain, liver, kidney, spleen, heart, testes, lung, and white (WAT) and brown (BAT) adipose tissue from vehicle and JZL184-treated mice. C57Bl/6 mice were treated with JZL184 at 16 mg kg^{-1} in saline-emulphor, sacrificed at 2 h, and their tissues were harvested. We detected a 33 kDa, JZL184-sensitive band by gel-based ABPP in every tissue proteome analyzed (Figure 4A–I). In brain and testes, a 35-kDa form of MAGL was also observed by gel-based ABPP, as reported previously [17, 20], perhaps reflecting an additional splice isoform of MAGL in these tissues [33]. Despite producing an equivalent and near-complete blockade of MAGL activity in each tissue (as judged by FP-rhodamine labeling), JZL184 inhibited 2-AG hydrolysis activity in these tissues to varying extents. For most tissues, a > 50% block of 2-AG hydrolysis activity was observed in JZL184-treated animals (Figure 4). BAT and WAT, however, showed only modest 30% decreases in activity (Figure 4F and G), possibly reflecting the action of other 2-AG hydrolases in these fat tissues, such as hormone-sensitive lipase, that are insensitive to JZL184.

Individual tissues showed markedly different extents and patterns of MAG accumulation following MAGL inhibition by JZL184. As reported previously, brain exhibited a dramatic (> 5-fold) increase in 2-AG levels, but more modest (~2-fold) increases in C16:0 and C18:1 MAGs. Liver, kidney, spleen, heart, and BAT showed significant ($P < 0.05$) elevations across the entire panel of MAG species analyzed, with the largest elevations being observed in the C16:0 and C18:1 species (Figure 4B–F). WAT and lung, on the other hand, did not show elevations in C20:4 MAG, but accumulated both C16:0 and C18:1 MAG (Figure 4G and H). Finally, despite the presence of MAGL in testes and its inactivation by JZL184 as judged by

ABPP and 2-AG hydrolysis assays, we did not observe any significant changes ($P > 0.05$) in any MAG species in this tissue (Figure 4I). We also did not observe any significant accumulation ($P > 0.05$) of AEA in any of the tissues in this analysis (Figure 4A–I). Lastly, we confirmed that JZL184 reduced arachidonic acid levels in brain (Table S1) as had been previously reported [18, 20], but found no changes in palmitic, stearic, oleic, or arachidonic acid in any of the peripheral tissues analyzed (Figure S5).

Selectivity profiling of JZL184 in peripheral mouse tissues

The pharmacological value of JZL184 for characterizing the physiological functions of MAGL depends on the selectivity of this inhibitor. Of the nine tissues analyzed by competitive ABPP from JZL184-treated mice, only spleen and lung contained detectable off-target(s), which migrated between 60–75 kDa. To further characterize these peripheral off-targets of JZL184, we analyzed lung membrane proteomes using an advanced liquid chromatography-mass spectrometry (LC-MS) platform, termed ABPP-MudPIT, that displays enhanced resolution and sensitivity compared to gel-based ABPP [34]. Briefly, lung membrane proteomes from mice treated with JZL184 or vehicle were subjected to competitive ABPP with the biotinlyated fluorophosphonate (FP) probe, FP-biotin [35]. FP-biotin-labeled proteins were then enriched with avidin, digested on-bead with trypsin, analyzed by multidimensional LC-MS, and identified and quantified using the SEQUEST search algorithm [36] and spectral counting [37], respectively. ABPP-MudPIT confirmed that JZL184 (16 mg kg^{-1} in saline-emulphor, i.p., 2 h) completely inhibited MAGL in lung membrane proteomes and also identified three additional targets of this compound, all from the carboxylesterase family: esterase 1 (ES1), esterase 1-like (ES1L), and carboxylesterase ML1 (also annotated as a second triglyceride hydrolase, TGH2 [38]) (Figure 5 and Table S2). The spectral count signals for hormone-sensitive lipase (HSL) were also lower in JZL184-treated lung proteomes, although this reduction did not reach statistical significance. To confirm whether these enzymes were valid targets of JZL184, we recombinantly expressed ES1, TGH2, and HSL in COS7 cells and evaluated them for sensitivity to JZL184 by competitive ABPP. JZL184 inhibited FP-rhodamine labeling of both ES1 and TGH2 (Figure 5) with potencies comparable to the inhibition of recombinant mouse MAGL [18,20]. In contrast, FP-rhodamine labeling of recombinant HSL was not impaired (Figure 5), confirming that this hydrolase is not a target of JZL184. Collectively, these functional proteomic data indicate that JZL184 maintains excellent selectivity for MAGL across most mouse tissues, targeting only a limited number of additional hydrolases in a subset of peripheral tissues.

JZL184 is equipotent against human and mouse MAGL, but less active against rat MAGL

To understand the scope of JZL184 activity against different MAGL orthologues, we recombinantly expressed mouse, rat, and human MAGL in COS7 cells and measured JZL184 inactivation of these enzymes *in vitro* by substrate assays (Figure 6A). JZL184 inhibited mouse and human MAGL with equal potency, but showed ~10-fold lower activity against rat MAGL (Figure 6B). We confirmed the lower potency of JZL184 against rat MAGL by *in vitro* competitive ABPP analysis of mouse and rat brain membranes (Figure 6C and D). JZL184 also appears to show a similar reduction in activity against rat FAAH, resulting in an overall similar relative selectivity windows for MAGL over FAAH in both mouse and rat brain proteomes (Figure 6D). Lastly, JZL184 showed equivalent potency against rat and mouse ABHD6 (Figure 6D), a second 2-AG hydrolase expressed in brain [17].

DISCUSSION

Despite its molecular characterization over a decade ago [2], the physiological functions of MAGL have remained relatively enigmatic due to a dearth of pharmacological tools or genetic models to test the enzyme's function in vivo. We recently introduced an efficacious and

selective inhibitor of MAGL, termed JZL184, and showed that this agent can selectively block MAGL activity in the nervous system of mice [18,20]. However, the mechanism by which JZL184 inhibits MAGL, as well as the scope of its inhibitory effect on MAGL in various tissues, remained unknown. Here, we provide clear evidence that JZL184 acts as a long-lasting irreversible inhibitor of MAGL by carbamoylating the enzyme's serine nucleophile. We furthermore show that JZL184 inactivates MAGL with good efficacy and selectivity in a wide range of central and peripheral tissues.

Interestingly, the impact of MAGL blockade on endocannabinoid/MAG metabolism differed markedly in individual tissues. In brain, both the basal level of 2-AG (5–10 nmol/g) and its fold-elevation following MAGL inhibition (> 5-fold) were much higher than in any peripheral tissue (Figure 4A). In contrast, several peripheral tissues from JZL184-treated mice accumulated substantial quantities of C16:0 and C18:1 MAGs (the two speices that were only modestly elevated in brain), while showing little or no elevation in 2-AG (Figure 4). These data, in addition to the high relative expression of CB1 in the brain compared to peripheral tissues [39] may suggest enhanced tonic levels of 2-AG metabolism and signaling in the nervous system compared to peripheral tissues. Conversely, the more dramatic elevations in C16:0 and C18:1 MAGs observed in some peripheral tissues following MAGL blockade may reflect a more general metabolic function for this enzyme at these sites. Another feature distinctive to MAGL in the nervous system is its regulation of brain arachidonic acid levels (Table S1), which was not observed in any peripheral tissues (Figure S5). These data again underscore differences in the function of MAGL in the brain and the periphery.

Because all tissues analyzed from JZL184-treated mice showed > 90% inhibition of MAGL as judged by gel-based ABPP (Figure 4), we presume that the distinct MAG profiles observed in individual tissues upon JZL184 treatment arise from other factors such as the presence of additional MAG hydrolases or different capacities for MAG biosynthesis. The former possibility seems likely in organs, such as WAT, where other enzymes that display MAG hydrolytic activity, such as HSL, are present at high levels [40,41]. The latter possibility is supported by preliminary time-course experiments, which have revealed similar relative rates of 2-AG accumulation in the brain and liver upon JZL184 treatment, but distinct plateau values for elevations in this endocannabinoid (11- and 4-fold, respectively) (Figure S5). Regardless of the precise mechanism, tissue-specific differences in endocannabinoid metabolism may help to explain the diversity of physiological functions performed by this lipid signaling system. Indeed, recent evidence suggests that CB1 antagonists affect metabolism, at least in part, by disrupting endocannabinoid pathways at peripheral sites such as liver [42] and adipocytes [43]. Determining how the local concentrations of endocannabinoids are regulated at these peripheral sites is critical to achieve a full understanding of the mechanism of action of these signaling lipids.

Our studies also point to two areas for future improvement of MAGL inhibitors. First, while competitive ABPP confirmed that JZL184 generally displays high selectivity for MAGL, a handful of additional targets were discovered in select peripheral tissues. That these "off-targets" corresponded to carboxylesterases is not surprising, given that other carbamates, such as the FAAH inhibitor URB597, have also been shown to inhibit carboxylesterases [24,31]. While we have previously demonstrated that JZL184 does not interact with other components of the endocannabinoid system [20], we cannot exclude the possibility that JZL184 interacts with other proteins outside of the serine hydrolase superfamily, such as cytochrome P450 enzymes, that may also participate in lipid metabolism [44]. Although the inhibition of carboxylesterases and other potential off-targets could complicate interpretation of JZL184's pharmacological effects in certain peripheral tissues, assessing the reversibility of observed effects by cannabinoid receptor antagonists should clarify whether they are due to the enhanced 2-AG signaling or a different mechanism. Regardless, having defined the principal off-targets

of JZL184 through functional proteomic profiling, we are in good position to move forward with directed medicinal chemistry efforts to improve the selectivity of this inhibitor. A second feature of JZL184 to consider for future refinement is species selectivity. JZL184 potently inhibited both mouse and human MAGL, but showed a 10-fold reduced activity against rat MAGL. Because rats are extensively used as a model system for studying higher order behaviors, it would be beneficial to develop inhibitors with improved activity against rat MAGL. However, this task may prove difficult to accomplish using the piperidine carbamate scaffold of JZL184, since our preliminary work with other inhibitors from this class have revealed a consistent trend toward higher potency for mouse and human MAGL over rat MAGL (our unpublished observations). Considering the high sequence identity shared by the three MAGL orthologues (92% between mouse and rat MAGL and 84% between mouse and human MAGL), we anticipate that structural studies may be required to clarify their surprising differences in sensitivity to JZL184 and related compounds.

SIGNIFICANCE

Monoacylglycerol lipase (MAGL) is a principal degradative enzyme for the endocannabinoid 2-arachidonoylglycerol (2-AG). Selective inhibitors of MAGL are therefore of value as both research tools to study the physiological functions of the endocannabinoid system and potential pharmaceutical agents to infiltrate this system for therapeutic gain. Here, we have shown that the piperidine carbamate JZL184 irreversibly inactivates MAGL by carbamoylation of the enzyme's catalytic serine nucleophile. This inhibition is observed *in vivo* with high selectivity in both central and peripheral tissues, enabling a comprehensive analysis of the contribution that MAGL makes to the metabolism of 2-AG and other monoglycerides. Interestingly, our studies provide evidence for marked tissue-specific differences in endocannabinoid tone, with brain showing the most dramatic elevations in 2-AG following MAGL blockade. In contrast, MAGL's control over the levels of 2-AG and other monoglycerides varied considerably in peripheral tissues, even in cases where this enzyme was largely responsible for bulk 2-AG hydrolytic activity. These data thus point to organs where MAGL-regulated 2-AG signaling may have its most profound effects on physiology and, conversely, to tissues where other enzymes might contribute to 2-AG and monoglyceride metabolism in vivo.

EXPERIMENTAL PROCEDURES

Materials

2-AG, d_5-2-AG, AEA, d_4-AEA, d_4-PEA, and pentadecanoic acid (PDA) were purchased from Cayman Chemicals. Monopentadecanoin and monoheptadecanoin were purachased from Nu-Chek-Prep, Inc. FP-rhodamine [29], FP-biotin [35], and JZL184 [20] were synthesized as described previously.

Expression and purification of recombinant MAGL and MAGL-S122A

Human MAGL was PCR amplified using the following primers: forward, GACTGGATCCCATGCCAGAGGAAAGTTC; reverse, CAGTAAGCTTTCAGGGTGGGGACGCAGTTC. The PCR product was subsequently cloned into pET-45b(+) (Novagen) using BamHI and HindIII restriction sites. The resulting hMAGL-pET45b(+) construct was transformed into BL21(DE3) cells (Invitrogen) for expression. A single colony from a fresh transformation was used to inoculate an overnight culture in a media of LB containing 100 μg ml^{-1} carbenicillin (LB^{carb}), incubated at 37°C with shaking (225 rpm). The following morning, the overnight culture was used to seed the induction culture at a ratio of 1:100. The induction culture was incubated at 37°C with shaking (225 rpm) and the OD_{600} was monitored each hour. Once the OD_{600} reached 0.4–0.6 1 mM IPTG was added each induction culture and allowed to incubate for additional 4 h. Cells were harvested

by centrifugation at 6000 × *g* for 10 min at 4°C. Cell pellets were stored at −80°C. To purify 6xHIS-hMAGL, cell pellets from a 1 liter culture were thawed at room temperature in a buffer containing 50 mM Tris (pH 8.0), 200 mM NaCl, 1% LDAO, lysozyme (0.25 mg ml^{-1}), and DNase I (25 μg ml^{-1}) with constant stirring for ~10 min, after which cells were lysed by sonication. The soluble and insoluble materials were separated by centrifugation at 24,000 × g for 30 min at 4°C. The resulting supernatant was batch loaded with 0.5 ml of TALON Metal Affinity Resin (Clontech) (50% slurry) for 1 h at 4°C. The loaded resin was added to a column and washed with 10 column volumes (CV) of 50 mM Tris pH 8.0, 200 mM NaCl (wash buffer), 10 CV of wash buffer containing with 5 mM imidazole, 10 CV of wash buffer containing 10 mM imidazole, and eluted with wash buffer containing with 200 mM imidazole. The eluted protein was subsequently concentrated using an Amicon Ultra centrifugal filter device (Millipore) with 10,000 molecular weight cut-off and the protein concentration determined using D_C Protein Assay (Bio-Rad). A typical 1 liter pellet (~1.5 g) will yield ~1.5 mg of MAGL of single band purity when analyzed by SDS-PAGE and stained with Coomassie Blue.

The MAGL-S122A construct was created using the following primers: sense, CTTCTGGGCCACGCCATGGGAGGCG; antisense, CGCCTCCCATGGCGTGGCCCAGAAG, and the Stratagene QuikChange II Site-Directed Mutagenesis kit according to the manufacturer's protocols.

LC-MS/MS detection of modified and unmodified tryptic peptides from JZL184-treated preparations of MAGL

Purified, recombinant hMAGL (50 μl, 5 mg ml^{-1}) was incubated with DMSO (1 μl) or JZL184 (1 μl, 200 μM final) for 20 min at room temperature. Urea (100 mg) was added to each reaction and the reactions were diluted with PBS (150 μl). Each sample was then subsequently incubated with *tris*-(2-carboxyethyl)phosphine (TCEP, 5 mM) and iodoacetamide (10 mM) for 30 min each at room temperature. The samples were diluted again with ammonium bicarbonate (25 mM, 550 μl) and subjected to trypsin digestion overnight at 37°C. The next day, samples were concentrated, resuspended in ammonium bicarbonate (25 mM, 200 μl) with 0.1% formic acid, and a 10 μl aliquot was pressue loaded onto a 100 μm (inner diameter) fused silica capillary column with a 5 μm tip that contained 10 cm of C18 resin (aqua 5 μm, Phenomenex). LC-MS/MS analysis was performed on an LTQ-Orbitrap mass spectrometer (ThermoFisher) coupled to an Agilent 1100 series HPLC. Peptides were eluted from the column using a 125-min gradient of 5–100% Buffer B (Buffer B: 20% water, 80% acetonitrile, 0.1% formic acid). The flow rate through the column was 0.25 μl min^{-1} and the spray voltage was 2.5 kV. The LTQ was operated in data-dependent scanning mode, with one full MS scan (400–1600 *m*/*z*) followed by seven MS/MS scans of the n^{th} most abundant ions with dynamic exclusion enabled.

Measurement of reversibility of JZL184-MAGL reaction

Recombinant mMAGL overexpressed in COS7 cells was diluted in Tris buffer (50 mM, pH 8, 1 mg ml^{-1} final concentration, 130 μl final volume) and was incubated with JZL184 (100 μM) or DMSO for 30 min at room temperature. The samples were then subjected to a PD10 size exclusion column (GE Healthcare), concentrated to 200 μl, and incubated at room temperature. At the indicated times, an aliquot of each sample was removed and substrate hydrolysis activity was determined exactly as described below.

Preparations of mouse and rat tissue proteomes

Tissues were Dounce-homogenized in PBS, pH 7.5, followed by a low-speed spin (1,400 × *g*, 5 min) to remove debris. The supernatant was then subjected to centrifugation (64,000 × *g*, 45 min) to provide the cytosolic fraction in the supernatant and the membrane fraction as a pellet. The pellet was washed and resuspended in PBS buffer by sonication. Total protein

concentration in each fraction was determined using a protein assay kit (Bio-Rad). Samples were stored at −80°C until use.

Competitive ABPP experiments

Tissue proteomes were diluted to 1 mg ml^{-1} in PBS and FP-rhodamine was added at a final concentration of 1 μM in a 50 μl total reaction volume. After 30 min at 25°C, the reactions were quenched with 4x SDS-PAGE loading buffer, boiled for 5 min at 90°C, subjected to SDS-PAGE and visualized in-gel using a flatbed fluorescence scanner (Hitachi). For experiments involving a pre-incubation with inhibitor, the reactions were prepared without FP-rhodamine. JZL184 was added at the indicated concentration and incubated for 30 min at 37°C. FP-rhodamine was then added and the reaction was carried out exactly as described above. For ABPP-MudPIT studies, a portion of the lung membrane proteome (0.5 ml, 1 mg ml^{-1} in PBS) from the mice treated with JZL184 or vehicle as described above was labeled with 5 μM FP-biotin for 2 h at room temperature and prepared for ABPP-MudPIT analysis as described previously [20,34], except that the Lys-C digestion step was omitted. MudPIT analysis of eluted peptides was carried out as previously described on a coupled Agilent 1100 LC-ThermoFinnigan LTQ-MS instrument. All data sets were searched against the mouse IPI database using the SEQUEST search algorithm [36] and the results were filtered and grouped with DTASELECT [45]. Peptides with cross-correlation scores greater than 1.8 (+1), 2.5 (+2), 3.5 (+3) and delta CN scores greater than 0.08 were included in the spectral counting analysis. Spectral counts are reported as the average of three samples with the standard error of the mean (SEM).

Recombinant expression of enzymes in COS7 cells

Enzymes were recombinantly expressed in COS7 using a previously described procedure [17] as detailed in the Supplemental Data.

Enzyme activity assays

MAGL and FAAH substrate hydrolysis assays were performed using previously described LC-MS assays [17] as detailed in the Supplemental Data.

In vivo studies with JZL184

JZL184 was prepared as a saline-emulphor emulsion by vortexing, sonicating, and gently heating neat compound directly into an 18:1:1 v/v/v solution of saline:ethanol:emulphor (4, 1.6, or 0.4 mg ml^{-1} final concentrations), or as a homogeneous PEG solution by vortexing, sonicating, and gently heating neat compound directly into PEG300 (Fluka) (4 mg ml^{-1} final concentration). Male C57Bl/6J mice (< 6 months old, 20–28 g) were intraperitoneally (i.p.) administered JZL184 or an 18:1:1 v/v/v saline:emulphor:ethanol vehicle at a volume of 10 μl g^{-1} weight (40, 16, or 4 mg kg^{-1} by the dilutions above) or a PEG vehicle at a volume of 4 μl g^{-1} weight (16 mg kg^{-1} by the dilution above). All experiments were performed with the saline-emulphor vehicle unless otherwise indicated. After the indicated amount of time, mice were anesthetized with isofluorane and killed by decapitation. Brains were removed, hemisected along the midsagittal plane, and each half was then flash frozen in liquid N_2. Two separate portions (~100 mg) of the other indicated tissues were also harvested and flash frozen in liquid N_2. One portion of each tissue was analyzed by gel-based ABPP and the other portion was used for metabolite analysis. Animal experiments were conducted in accordance with the guidelines of the Institutional Animal Care and Use Committee of The Scripps Research Institute.

Measurement of brain lipids

Brain lipid measurements were determined using a slight modification from a previously described procedure [20] as detailed in the Supplemental Data.

Mouse behavioral experiments

Locomotor activity was assessed in a Plexiglas cage (18 × 10 × 8.5 in) that was marked by 7 cm × 7 cm grids on the bottom of the cage. The number of grids traversed by the hind limbs was counted for 5 minutes. Nociception was then assessed in the tail immersion assay, where each mouse was hand-held and 1 cm of the tail was submerged into a 56°C water bath. The latency for the mouse to withdrawal its tail was scored. Rectal temperature was assessed by inserting a thermocouple probe 1.2 cm into the rectum and temperature was determined using a telethermometer. Pre-injection tail immersion latency and rectal temperature was also measured as a baseline for each mouse.

Supplementary Material

Refer to Web version on PubMed Central for supplementary material.

Acknowledgments

We thank Tianyang Ji for assistance with the transfection of MAGL cDNAs, Jason R. Thomas for purified human MAGL, and the Cravatt lab for helpful discussion and critical reading of the manuscript. This work was supported by the US National Institutes of Health (DA017259), the Helen L. Dorris Institute Child and Adolescent Neuro-Psychiatric Disorder Institute, and the Skaggs Institute for Chemical Biology.

References

1. Tornqvist H, Belfrage P. Purification and some properties of a monoacylglycerol-hydrolyzing enzyme of rat adipose tissue. Journal of Biological Chemistry 1976;251:813–819. [PubMed: 1249056]
2. Karlsson M, Contreras JA, Hellman U, Tornqvist H, Holm C. cDNA cloning, tissue distribution, and identification of the catalytic triad of monoglyceride lipase. Evolutionary relationship to esterases, lysophospholipases, and haloperoxidases. Journal of Biological Chemistry 1997;272:27218–27223. [PubMed: 9341166]
3. Fredrikson G, Tornqvist H, Belfrage P. Hormone-sensitive lipase and monoacylglycerol lipase are both required for complete degradation of adipocyte triacylglycerol. Biochimica et Biophysica Acta 1986;876:288–293. [PubMed: 3955067]
4. Sugiura T, Kondo S, Sukagawa A, Nakane S, Shinoda A, Itoh K, Yamashita A, Waku K. 2-Arachidonoylglycerol: a possible endogenous cannabinoid receptor ligand in brain. Biochemical and Biophysical Research Communications 1995;215:89–97. [PubMed: 7575630]
5. Mechoulam R, Ben-Shabat S, Hanus L, Ligumsky M, Kaminski NE, Schatz AR, Gopher A, Almog S, Martin BR, Compton DR, et al. Identification of an endogenous 2-monoglyceride, present in canine gut, that binds to cannabinoid receptors. Biochemical Pharmacology 1995;50:83–90. [PubMed: 7605349]
6. Dinh TP, Carpenter D, Leslie FM, Freund TF, Katona I, Sensi SL, Kathuria S, Piomelli D. Brain monoglyceride lipase participating in endocannabinoid inactivation. Proceedings of the National Academy of Sciences of the United States of America 2002;99:10819–10824. [PubMed: 12136125]
7. Devane WA, Hanus L, Breuer A, Pertwee RG, Stevenson LA, Griffin G, Gibson D, Mandelbaum A, Etinger A, Mechoulam R. Isolation and structure of a brain constituent that binds to the cannabinoid receptor. Science 1992;258:1946–1949. [PubMed: 1470919]
8. Matsuda LA, Lolait SJ, Brownstein MJ, Young AC, Bonner TI. Structure of a cannabinoid receptor and functional expression of the cloned cDNA. Nature 1990;346:561–564. [PubMed: 2165569]
9. Munro S, Thomas KL, Abu-Shaar M. Molecular characterization of a peripheral receptor for cannabinoids. Nature 1993;365:61–65. [PubMed: 7689702]

10. Mackie K. Cannabinoid receptors as therapeutic targets. Annual Review of Pharmacology and Toxicology 2006;46:101–122.
11. Ledent C, Valverde O, Cossu G, Petitet F, Aubert JF, Beslot F, Bohme GA, Imperato A, Pedrazzini T, Roques BP, Vassart G, Fratta W, Parmentier M. Unresponsiveness to cannabinoids and reduced addictive effects of opiates in CB1 receptor knockout mice. Science 1999;283:401–404. [PubMed: 9888857]
12. Zimmer A, Zimmer AM, Hohmann AG, Herkenham M, Bonner TI. Increased mortality, hypoactivity, and hypoalgesia in cannabinoid CB1 receptor knockout mice. Proceedings of the National Academy of Sciences of the United States of America 1999;96:5780–5785. [PubMed: 10318961]
13. Di Marzo V, Bisogno T, De Petrocellis L. Endocannabinoids and Related Compounds: Walking Back and Forth between Plant Natural Products and Animal Physiology. Chemistry & Biology 2007;14:741–756. [PubMed: 17656311]
14. Cravatt BF, Giang DK, Mayfield SP, Boger DL, Lerner RA, Gilula NB. Molecular characterization of an enzyme that degrades neuromodulatory fatty-acid amides. Nature 1996;384:83–87. [PubMed: 8900284]
15. Cravatt BF, Demarest K, Patricelli MP, Bracey MH, Giang DK, Martin BR, Lichtman AH. Supersensitivity to anandamide and enhanced endogenous cannabinoid signaling in mice lacking fatty acid amide hydrolase. Proceedings of the National Academy of Sciences of the United States of America 2001;98:9371–9376. [PubMed: 11470906]
16. Dinh TP, Kathuria S, Piomelli D. RNA interference suggests a primary role for monoacylglycerol lipase in the degradation of the endocannabinoid 2-arachidonoylglycerol. Molecular Pharmacology 2004;66:1260–1264. [PubMed: 15272052]
17. Blankman JL, Simon GM, Cravatt BF. A comprehensive profile of brain enzymes that hydrolyze the endocannabinoid 2-arachidonoylglycerol. Chemistry and Biology 2007;14:1347–1356. [PubMed: 18096503]
18. Nomura DK, Hudak CS, Ward AM, Burston JJ, Issa RS, Fisher KJ, Abood ME, Wiley JL, Lichtman AH, Casida JE. Monoacylglycerol lipase regulates 2-arachidonoylglycerol action and arachidonic acid levels. Bioorganic and Medicinal Chemistry Letters 2008;18:5875–5878. [PubMed: 18752948]
19. Nomura DK, Blankman JL, Simon GM, Fujioka K, Issa RS, Ward AM, Cravatt BF, Casida JE. Activation of the endocannabinoid system by organophosphorus nerve agents. Nat Chem Biol 2008;4:373–378. [PubMed: 18438404]
20. Long JZ, Li W, Booker L, Burston JJ, Kinsey SG, Schlosburg JE, Pavon FJ, Serrano AM, Selley DE, Parsons LH, Lichtman AH, Cravatt BF. Selective blockade of 2-arachidonoylglycerol hydrolysis produces cannabinoid behavioral effects. Nat Chem Biol 2009;5:37–44. [PubMed: 19029917]
21. Li W, Blankman JL, Cravatt BF. A functional proteomic strategy to discover inhibitors for uncharacterized hydrolases. Journal of the American Chemical Society 2007;129:9594–9595. [PubMed: 17629278]
22. Leung D, Hardouin C, Boger DL, Cravatt BF. Discovering potent and selective reversible inhibitors of enzymes in complex proteomes. Nature Biotechnology 2003;21:687–691.
23. Bar-On P, Millard CB, Harel M, Dvir H, Enz A, Sussman JL, Silman I. Kinetic and structural studies on the interaction of cholinesterases with the anti-Alzheimer drug rivastigmine. Biochemistry 2002;41:3555–3564. [PubMed: 11888271]
24. Alexander JP, Cravatt BF. Mechanism of carbamate inactivation of FAAH: implications for the design of covalent inhibitors and in vivo functional probes for enzymes. Chemistry and Biology 2005;12:1179–1187. [PubMed: 16298297]
25. Verty AN, Singh ME, McGregor IS, Mallet PE. The cannabinoid receptor antagonist SR 141716 attenuates overfeeding induced by systemic or intracranial morphine. Psychopharmacology 2003;168:314–323. [PubMed: 12700881]
26. Lichtman AH, Sheikh SM, Loh HH, Martin BR. Opioid and cannabinoid modulation of precipitated withdrawal in delta9-THC and morphine-dependent mice. J Pharmacol Exp Ther. 2001 in press.
27. Fegley D, Gaetani S, Duranti A, Tontini A, Mor M, Tarzia G, Piomelli D. Characterization of the fatty acid amide hydrolase inhibitor cyclohexyl carbamic acid 3′-carbamoyl-biphenyl-3-yl ester (URB597): effects on anandamide and oleoylethanolamide deactivation. Journal of Pharmacology and Experimental Therapeutics 2005;313:352–358. [PubMed: 15579492]

28. Naidu PS, Booker L, Cravatt BF, Lichtman AH. Synergy between enzyme inhibitors of fatty acid amide hydrolase and cyclooxygenase in visceral nociception. Journal of Pharmacology and Experimental Therapeutics. 2009
29. Patricelli MP, Giang DK, Stamp LM, Burbaum JJ. Direct visualization of serine hydrolase activities in complex proteomes using fluorescent active site-directed probes. Proteomics 2001;1:1067–1071. [PubMed: 11990500]
30. Ahn K, Johnson DS, Mileni M, Beidler D, Long JZ, McKinney MK, Weerapana E, Sadagopan N, Liimatta M, Smith SE, Lazerwith S, Stiff C, Kamtekar S, Bhattacharya K, Zhang Y, Swaney S, Van Becelaere K, Stevens RC, Cravatt BF. Discovery and characterization of a highly selective FAAH inhibitor that reduces inflammatory pain. Chemistry and Biology 2009;16:411–420. [PubMed: 19389627]
31. Zhang D, Saraf A, Kolasa T, Bhatia P, Zheng GZ, Patel M, Lannoye GS, Richardson P, Stewart A, Rogers JC, Brioni JD, Surowy CS. Fatty acid amide hydrolase inhibitors display broad selectivity and inhibit multiple carboxylesterases as off-targets. Neuropharmacology 2007;52:1095–1105. [PubMed: 17217969]
32. Ahn K, Johnson DS, Fitzgerald LR, Liimatta M, Arendse A, Stevenson T, Lund ET, Nugent RA, Nomanbhoy TK, Alexander JP, Cravatt BF. Novel mechanistic class of fatty acid amide hydrolase inhibitors with remarkable selectivity. Biochemistry 2007;46:13019–13030. [PubMed: 17949010]
33. Karlsson M, Reue K, Xia YR, Lusis AJ, Langin D, Tornqvist H, Holm C. Exon-intron organization and chromosomal localization of the mouse monoglyceride lipase gene. Gene 2001;272:11–18. [PubMed: 11470505]
34. Jessani N, Niessen S, Wei BQ, Nicolau M, Humphrey M, Ji Y, Han W, Noh DY, Yates JR 3rd, Jeffrey SS, Cravatt BF. A streamlined platform for high-content functional proteomics of primary human specimens. Nat Methods 2005;2:691–697. [PubMed: 16118640]
35. Liu Y, Patricelli MP, Cravatt BF. Activity-based protein profiling: the serine hydrolases. Proceedings of the National Academy of Sciences of the United States of America 1999;96:14694–14699. [PubMed: 10611275]
36. Eng JK, McCormack AL, Yates JR. An approach to correlate tandem mass spectral data of peptides with amino acid sequences in a protein database. Journal of the American Society for Mass Spectrometry 1994;5:976–989.
37. Liu H, Sadygov RG, Yates JR 3rd. A model for random sampling and estimation of relative protein abundance in shotgun proteomics. Anal Chem 2004;76:4193–4201. [PubMed: 15253663]
38. Okazaki H, Igarashi M, Nishi M, Tajima M, Sekiya M, Okazaki S, Yahagi N, Ohashi K, Tsukamoto K, Amemiya-Kudo M, Matsuzaka T, Shimano H, Yamada N, Aoki J, Morikawa R, Takanezawa Y, Arai H, Nagai R, Kadowaki T, Osuga J, Ishibashi S. Identification of a novel member of the carboxylesterase family that hydrolyzes triacylglycerol: a potential role in adipocyte lipolysis. Diabetes 2006;55:2091–2097. [PubMed: 16804080]
39. Mackie K. Distribution of cannabinoid receptors in the central and peripheral nervous system. Handb Exp Pharmacol 2005:299–325. [PubMed: 16596779]
40. Fredrikson G, Belfrage P. Positional specificity of hormone-sensitive lipase from rat adipose tissue. Journal of Biological Chemistry 1983;258:14253–14256. [PubMed: 6643478]
41. Osuga J, Ishibashi S, Oka T, Yagyu H, Tozawa R, Fujimoto A, Shionoiri F, Yahagi N, Kraemer FB, Tsutsumi O, Yamada N. Targeted disruption of hormone-sensitive lipase results in male sterility and adipocyte hypertrophy, but not in obesity. Proceedings of the National Academy of Sciences of the United States of America 2000;97:787–792. [PubMed: 10639158]
42. Osei-Hyiaman D, Liu J, Zhou L, Godlewski G, Harvey-White J, Jeong WI, Batkai S, Marsicano G, Lutz B, Buettner C, Kunos G. Hepatic CB1 receptor is required for development of diet-induced steatosis, dyslipidemia, and insulin and leptin resistance in mice. Journal of Clinical Investigation 2008;118:3160–3169. [PubMed: 18677409]
43. Motaghedi R, McGraw TE. The CB1 endocannabinoid system modulates adipocyte insulin sensitivity. Obesity (Silver Spring) 2008;16:1727–1734. [PubMed: 18551116]
44. Chen JK, Chen J, Imig JD, Wei S, Hachey DL, Guthi JS, Falck JR, Capdevila JH, Harris RC. Identification of novel endogenous cytochrome p450 arachidonate metabolites with high affinity for

cannabinoid receptors. Journal of Biological Chemistry 2008;283:24514–24524. [PubMed: 18606824]

45. Tabb DL, McDonald WH, Yates JR 3rd. DTASelect and Contrast: tools for assembling and comparing protein identifications from shotgun proteomics. J Proteome Res 2002;1:21–26. [PubMed: 12643522]

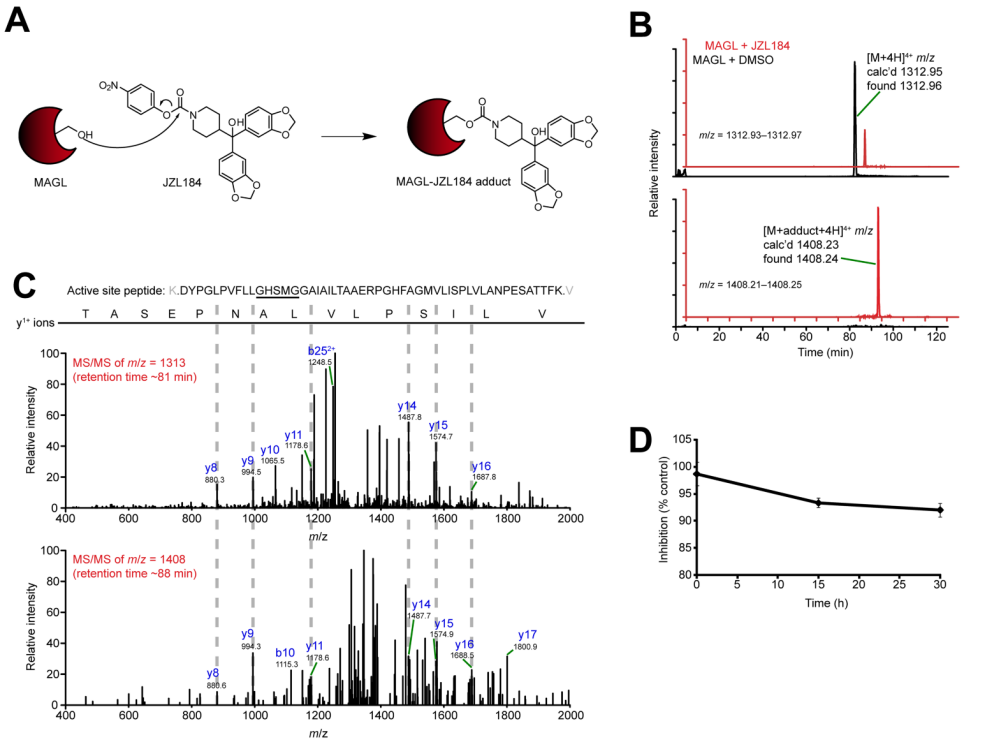

Figure 1.

Mechanism of JZL184 inhibition of MAGL. (A) Proposed mechanism for covalent inactivation of MAGL by JZL184 involving carbamoylation of the enzyme's catalytic serine nucleophile (Ser122). (B) Extracted ion chromatograms (EIC) of the unmodified (top) and JZL184-modified (bottom) MAGL active site tryptic peptide (amino acids 110–160). Recombinant, purified human MAGL was treated with DMSO (black trace) or JZL184 (200 μM, red trace). The mass window for each EIC, the detected high-resolution mass for each peak, and the charge state for each tryptic peptide are indicated. (C) MS/MS spectra generated by the unmodified and modified active site peptides. Diagnostic y and b ions are identified. All ions are in the 1 + charge state unless otherwise indicated. (D) JZL184-treated MAGL was incubated at room temperature in 50 mM Tris, pH 8.0, and the activity remaining as a percentage of control reactions (treated with DMSO) was measured by 2-AG hydrolysis assays. For (D), data are presented as means ± SEM of three independent experiments.

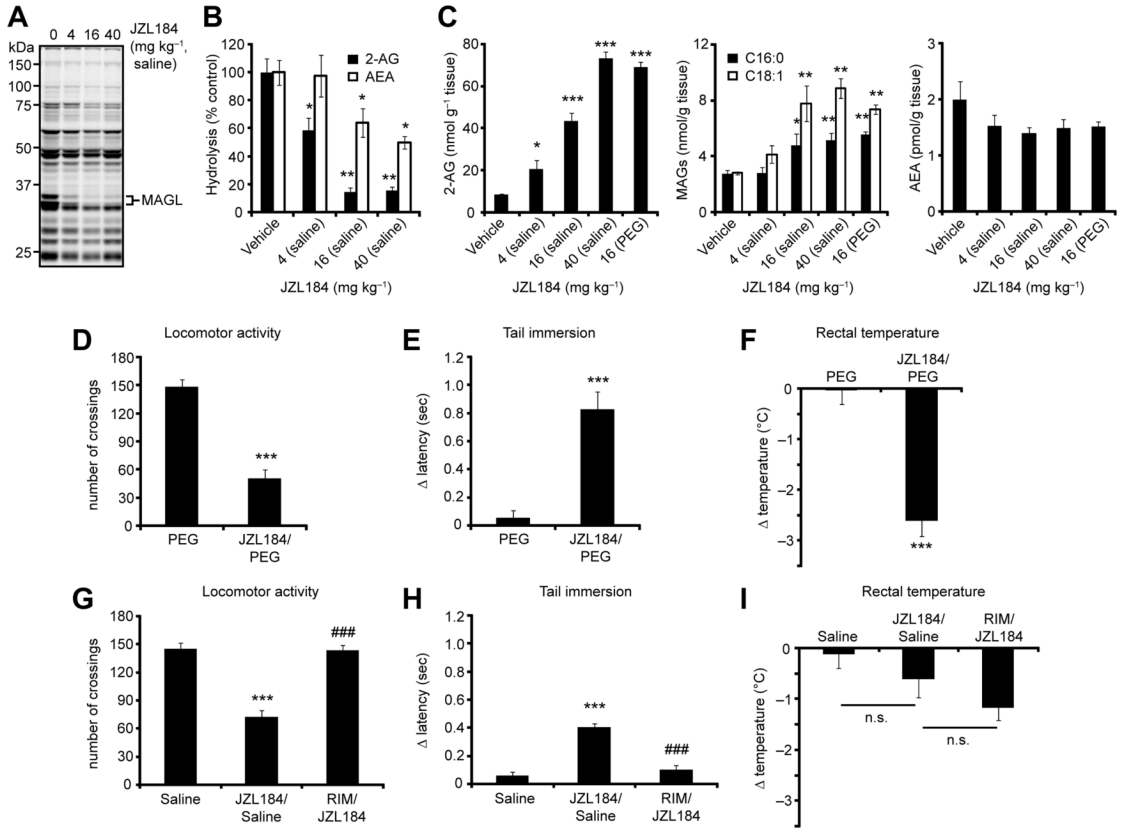

Figure 2.

Comparison of vehicles for JZL184 administration to mice. (A, B) Serine hydrolase activity profiles as determined by reactivity with the ABPP probe FP-rhodamine (A, fluorescent gel shown in grayscale) and 2-AG and AEA hydrolysis activity assays (B) of brain membranes prepared from mice treated with JZL184 (saline-emulphor, i.p., 4–40 mg kg^{-1}, 4 h). (C) Total brain 2-AG, PG (C16:0), OG (C18:1), and AEA measurements from mice treated with JZL184 (4–40 mg kg^{-1}) in the indicated vehicle for 4 h. (D–I). Locomotor activity (D, G), thermal pain sensation (E, H), and rectal temperature (F, I) of mice treated with JZL184 in the PEG (16 mg kg^{-1}, i.p., 4 h; *upper panels*) or saline-emulphor (40 mg kg^{-1}, i.p., 4 h; *lower panels*) vehicle. Mice in either treatment group were not cataleptic. Administration of the CB1 antagonist rimonabant (RIM, i.p., 3 mg kg^{-1}) to mice 15 min prior to JZL184 treatment blocked the observed behavioral effects in the saline-emulphor group (D–F, lower panels). RIM had been previously shown to block the behavioral effects of JZL184 administered in the PEG vehicle [20]. * $P < 0.05$, ** $P < 0.01$, *** $P < 0.001$ for inhibitor-treated versus vehicle-treated animals. ### $P < 0.001$ for RIM- and inhibitor-treated versus inhibitor-treated animals. Data are presented as means ± SEM; For (B) and (C), n = 3–6/group; for (D F), n = 10–18/group.

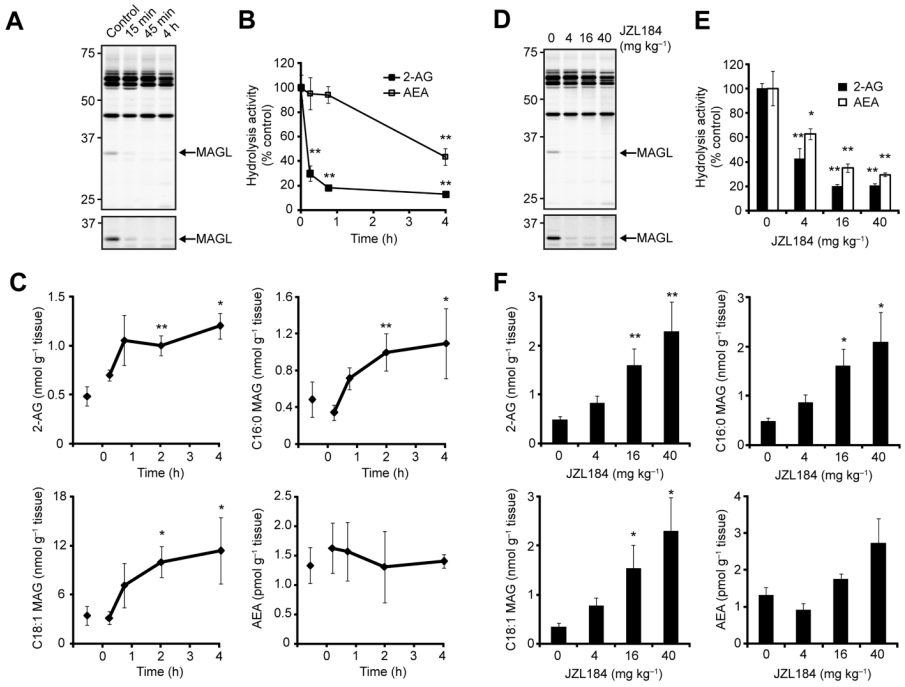

Figure 3.

Time course and dose-response analysis of MAGL inactivation by JZL184 in liver. (A, B) Serine hydrolase activity profiles as judged by FP-rhodamine labeling (A) and 2-AG and AEA hydrolysis assays (B) of liver membranes from mice treated with JZL184 (16 mg kg^{-1} in saline-emulphor, i.p.) for the indicated times. (C) Liver 2-AG (C20:4), PG (C16:0), OG (C18:1), and AEA levels from mice treated with JZL184 (16 mg kg^{-1} in saline-emulphor, i.p.) for the indicated times. (D, E) Serine hydrolase activity profiles (D) and 2-AG and AEA hydrolysis assays (E) of liver membranes from mice treated with JZL184 at the indicated doses (4–40 mg kg^{-1}, i.p.) for 4 h. (F) Liver 2-AG (C20:4), PG (C16:0), OG (C18:1), and AEA levels from mice treated with JZL184 at the indicated doses (4–40 mg kg^{-1} in saline-emulphor, i.p., 4 h). * $P < 0.05$, ** $P < 0.01$ for inhibitor-treated versus vehicle-treated animals. Data are presented as means ± SEM; $n = 3–4$/group.

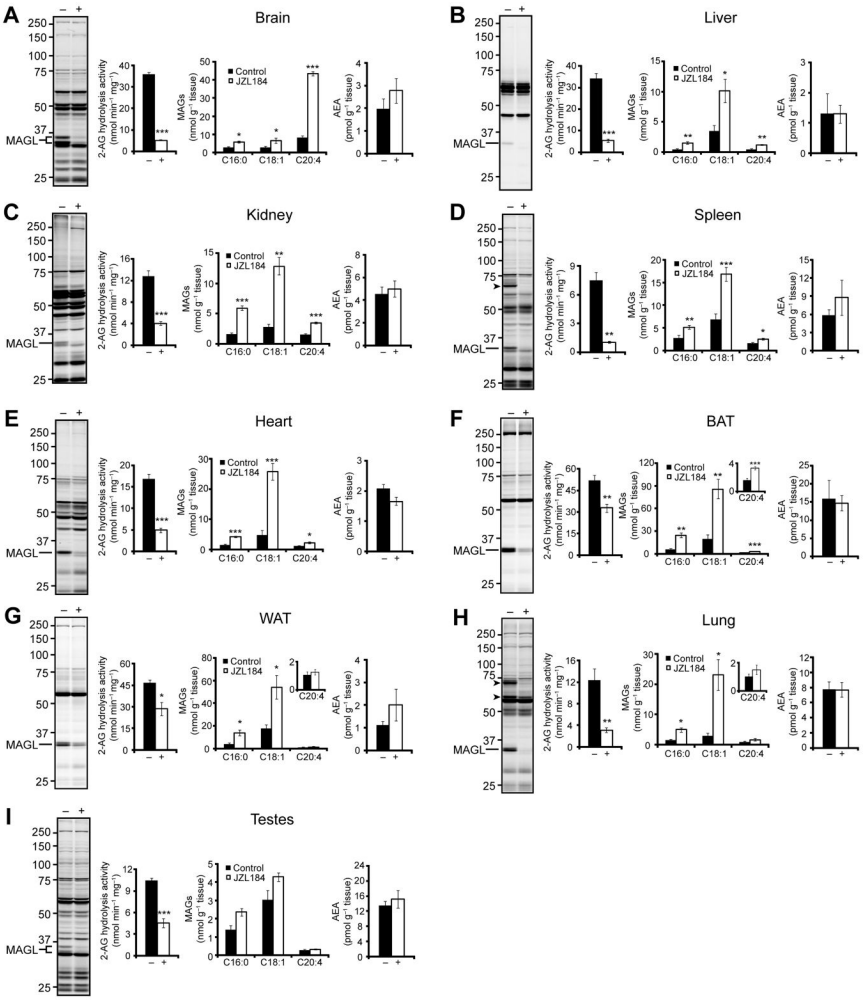

Figure 4.

A comprehensive biochemical profile of MAGL inactivation in tissues for JZL184-treated mice. (A–I) Serine hydrolase activity profiles as judged by FP-rhodamine labeling, 2-AG hydrolysis activity, and levels of MAGs and AEA in brain (A), liver (B), kidney (C), spleen (D), heart (E), brown adipose tissue (BAT) (F), white adipose tissue (WAT) (G), lung (H), and testes (I) from mice treated with JZL184 (16 mg kg^{-1} in saline-emulphor, i.p., 2 h). JZL184 off-targets are indicated by arrowheads. The 2 h metabolic data for liver is from the time course analysis presented in Figure 2C. * $P < 0.05$, ** $P < 0.01$, *** $P < 0.001$ for inhibitor-treated versus vehicle-treated animals. Data are presented as means ± SEM; $n = 4–6$/group.

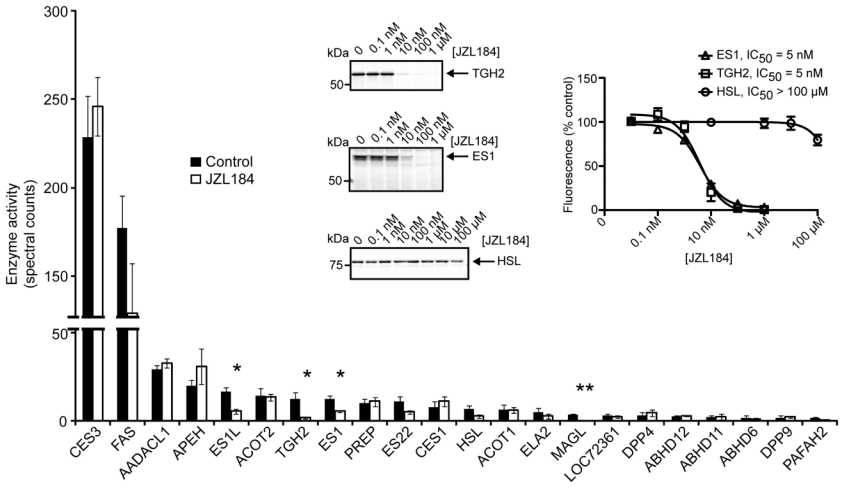

Figure 5.

ABPP-MudPIT analysis of lung membrane proteomes from mice treated with JZL184 (16 mg kg^{-1}, i.p., 2 h). Insert, Competitive ABPP measuring JZL184 blockade of FP-rhodamine for ES1, TGH2, and HSL recombinantly expressed in COS7 cells (left insert, representative competitive ABPP gels; right insert, quantification of blockade of FP-rhodamine labeling). Data are presented as means ± SEM of three independent experiments. * $P < 0.05$, ** $P < 0.01$, for inhibitor-treated versus vehicle-treated animals.

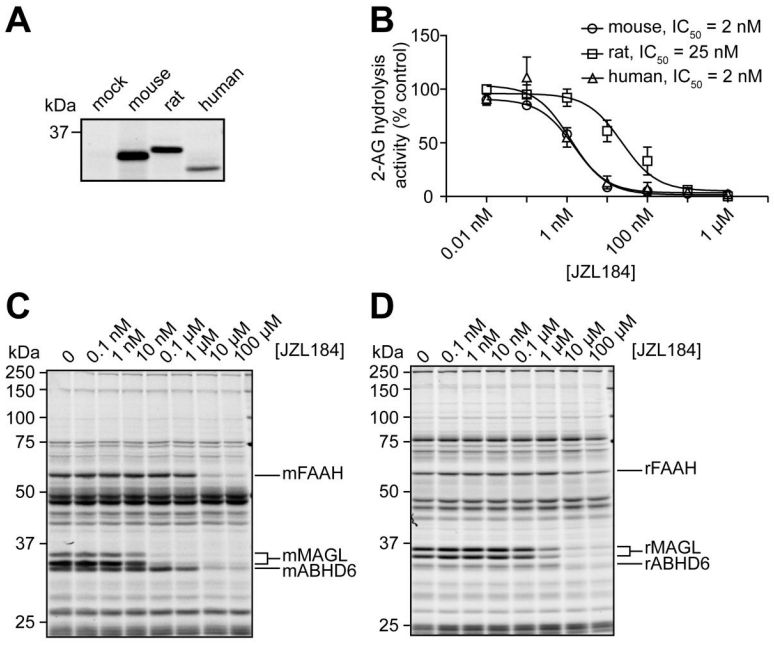

Figure 6.

Characterization of JZL184 inhibition of mouse, rat, and human MAGL. (A) FP-rhodamine labeling of recombinant mouse, rat, and human MAGL expressed in COS7 cells (1 μM FP-rhodamine, 30 min). (B) Blockade of recombinant MAGL orthologues by JZL184 as determined by substrate assays with 2-AG. Data are presented as means ± SEM of three independent experiments. (C, D) Competitive ABPP showing the effect of JZL184 on serine hydrolase activities in the mouse (C) and rat (D) brain membrane proteomes. For B–D, JZL184 was incubated with cell/tissue lysates (30 min, 37 °C) at the indicated concentrations, followed by addition of 2-AG (100 μM, 5 min, room temperature) (B) or FP-rhodamine (1 μM, 30 min, room temperature) (C, D). For (C, D), control proteomes were treated with DMSO alone. Note that mouse and rat brain MAGL migrates as a 33 and 35 kDa doublet by SDS-PAGE, as reported previously [17,20].